NBSIR 85-3201

Validation Test of An Earth Contact Heat Transfer Algorithm

George N. Walton

U.S. DEPARTMENT OF COMMERCE
National Bureau of Standards
National Engineering Laboratory
Center for Building Technology
Building Physics Division
Gaithersburg, MD 20899

October 1985

Prepared for:
Solar Buildings Technology Division
of Solar Heat Technology
epartment of Energy
gton, DC 20585

NBSIR 85-3201

VALIDATION TESTS OF AN EARTH CONTACT HEAT TRANSFER ALGORITHM

George N. Walton

U.S. DEPARTMENT OF COMMERCE
National Bureau of Standards
National Engineering Laboratory
Center for Building Technology
Building Physics Division
Gaithersburg, MD 20899

October 1985

Prepared for:
Solar Buildings Technology Division
Office of Solar Heat Technology
U.S. Department of Energy
Washington, DC 20585

U.S. DEPARTMENT OF COMMERCE, Malcolm Baldrige, *Secretary*
NATIONAL BUREAU OF STANDARDS, Ernest Ambler, *Director*

ABSTRACT

Experimental tests and numerical calculations are performed to determine the suitability of including a simplified earth contact heat transfer algorithm in building energy analysis computer simulations. Reasonable agreement is shown between the finite difference test program and the simplified method. There is very good agreement between the floor surface temperature of the NBS Passive Solar Test Facility and the temperature predicted by the test program. These results indicate that simplifications based upon the specific configuration can give good results for a simple calculation of the annual earth contact heat flux. There may be considerable differences in the hourly and daily heat flux values when the actual weather departs from the annual harmonic approximation of the simple method. A procedure is developed for using two-dimensional (2-D) simulation to closely approximate the full 3-D effects of heat transfer from rectangular basements and slabs. The 2-D method can be applied to other numerical procedures for which use a 2-D method for computing earth contact heat flux. It is recommended that any algorithm used in a large building energy analysis computer program include the capability of modeling the specific geometry under consideration instead of (or in addition to) using tables of coefficients which have been generated for a manual method. The algorithm should also include the ability to handle the same weather data that is used in the energy analysis.

TABLE OF CONTENTS

LIST OF TABLES

LIST OF FIGURES

1. INTRODUCTION

Earth contact heat transfer for basement and slab-on-grade floors is a major component of the heat balance in many buildings, particularly residences, and therefore significantly affects the heating and cooling energy consumption. This earth contact heat transfer is particularly important in mild climate zones. Most exiting building energy analysis programs estimate this earth contact heat transfer in very crude manners [1, 2, 3] even though they have very detailed calculations for many of the other heat transfer phenomena in buildings.

Detailed analysis of ground heat transfer is very difficult. It requires two- and in some case three-dimensional heat transfer analysis which, although not conceptually difficult, usually requires very time consuming calculations. The time scale of ground heat transfer is much longer than all other building phenomena, and it is difficult to combine both long and short time scale phenomena efficiently. The greatest difficulties occur with the ground thermal properties which are not constant and are often unknown at a particular site. Moisture is the primary factor in changing soil properties. It is dependent on local conditions of rainfall, drainage, and groundwater level, and it has a profound effect during freezing and thawing cycles.

Several approaches have been tried in developing tools for estimating earth contact heat transfer. A mathematically analytic method is used in reference [4] which solves a slab-on-grade configuration with constant thermal properties. The highly simplified geometry is characteristic of most analytic methods. Two-dimensional finite element or finite difference conduction calculations are often employed [5, 6, 7]. These numerical methods allow, but do not always use, more complex configurations and variable thermal properties. Another approach is to establish correlations based on purely experimental measurements of the ground heat flux as is done in [8] for basements. In each of the above cases, the method is used to develop a simplified approach (each of which is different from the others) allowing manual calculation of annual and/or peak heat loss from basements or slabs.

A recently published report by Mitalas [9] describes another technique for estimating earth contact heat transfer. It employes finite element calculations to establish sets of "conduction shape factors" for various earth contact configurations. Three dimensional effects are accounted for by "corner factors". Heat fluxes are computed monthly for the several sections of the earth contact surface. The final simplified calculation method provides enough detail in the time and spatial description of the heat transfer to be included as a subroutine in one of the more detailed building energy analysis programs. Although not all configurations are, or can be, included in a set of tables, the procedure exists for developing building specific shape factors.

This report will discuss tests of the Mitalas method using both numerical simulations and experimental data from a building with a slab-on-grade floor.

2. METHODS

2.1 THE MITALAS GROUND HEAT TRANSFER ALGORITHM

The Mitalas method is based on a finite element calculation which determines the conduction shape factors from several segments of a building's earth contact surface. These shape factors are used for computing earth contact heat transfer in much the same way as the U-value is used in computing one-dimensional heat transfer through walls. Figure 1 shows the six elements involved in heat loss from a basement: the outside environment, the basement wall and floor below grade, the ground surface, the lower thermal boundary, and the conducting soil between the basement, the ground surface, and the lower thermal boundary. The model assumes that the lower thermal boundary of the soil is at a constant temperature equal to the mean ground temperature and that the two vertical boundaries are adiabatic.

The walls are divided into five segments:

A1 = inside surface area of the basement wall above grade,

A2 = upper inside surface strip (0.6 m wide) of the wall below grade,

A3 = lower inside surface area of the wall below grade,

A4 = inside surface area of a floor strip 1 m wide adjacent to the wall,

A5 = inside surface area of the remainder of the floor.

The wall below grade and the floor are both divided into two segments because calculations show significant variations in the heat flux over the entire basement wall and floor. A slab-on-grade configuration would consist of segments A1, A4, and A5.

The total instantaneous heat loss from the basement is equal to the sum of the heat losses through all segments. The heat loss in each segment is given by the area of the segment times the instantaneous heat flux. The instantaneous heat flux in segment n, $Q_n(t)$, is approximated by

$$q_n(t) = q_{a,n} + q_{v,n} \cdot \sin(t) \qquad (1)$$

where $q_{a,n}$ = annual mean value of $q_n(t)$,

$q_{v,n}$ = amplitude of the first harmonic of the heat flux variation,

ω = angular velocity of the first harmonic,

t = time.

The two components of $q_n(t)$ in eq (1) can be expressed as

$$q_{a,n}(t) = S_n \cdot (\theta_B - \theta_G) \qquad (2)$$

and

$$q_{v,n}(t) = V_n \cdot \sigma_n \cdot \theta_v \cdot \sin(\omega(t+\Delta t_n)) \qquad (3)$$

where S_n = shape factor for the steady-state heat loss component,

θ_B = basement air temperature,

θ_G = ground surface temperature averaged over time and area,

V_n = shape factor for the periodic heat loss,

σ_n = amplitude attenuation factor,

θ_v = amplitude of the first harmonic of the ground surface temperature,

Δt_n = time lag of the heat flux relative to the surface temperature.

The shape factor, S_n, represents the overall conductance between the basement interior surface segment n (including the surface heat transfer coefficient) and the two boundaries: the ground surface and the deep ground plane. That is, $S_n = S_{n,s} + S_{n,g}$, where $S_{n,s}$ is conductance to the ground surface and $S_{n,g}$ is conductance to the hypothetical lower boundary plane which is at mean ground temperature. The shape factor, V_n, represents the overall conductance for periodic heat flow between the basement interior surface segment n and the ground surface. Therefore, V_n equals $S_{n,s}$. Note that the shape factors differ from a conventional shape factor which is dependent only on geometry and is independent of thermal conductivity.

Basement insulation is handled by modifying the shape factors according to

$$S_n(R) = 1/(a_n + b_n \cdot R) \quad (4)$$

and

$$V_n(R) = 1/(c_n + d_n \cdot R) \quad (5)$$

where $S_n(R)$ and $V_n(R)$ = S and V for a basement insulated with a thermal resistance of R.

a_n, b_n, c_n, d_n = constants specific to the basement insulation configuration.

The coefficients for S_n and V_n for many basement insulation configurations and two different soil conductivity values are given in table 2 of [9]. These coefficients are based on interior surface heat flux profiles calculated by finite-element numerical methods for heat conduction. The attentuation factor, σ_n, and the time-lag factor, Δt_n, are based on a sine wave variation of the ground surface temperature. Experimental studies have indicated that the variation in basement heat loss can be adequately described by monthly mean values of the basement heat loss. Therefore, the Mitalas method uses a time increment of one month with an angular velocity of 30 degrees per month. In order to account for the three-dimensional nature of the basement heat loss, a set of corner factors, C_n, was derived based on two levels of basement insulation.

Several factors cannot be taken directly into account by this model:

- the time variation in temperature and level of groundwater,

- the flow of rain or into the soil,

- the spatial variation of ground surface temperature around a basement due to solar effects, adjacent buildings, ground cover, and snowcover,

- the difference in thermal properties of backfill and undisturbed soil and of soil above and below the freezing plane.

When the permeability of the soil as a porous medium saturated with ground water is high enough, in addition to the thermal conduction estimates one has to take into account the contribution due to thermal convection. Poulikakos and Bejan [10] indicate that convection is not negligible when $Ra_\lambda^{1/3} >> 1$, where Ra_λ is the Darcy-modified Rayleigh number and λ is the horizontal length scale of the building. This relation serves as one constraint on the validity of the pure conduction models mentioned in this paper.

2.2 THE FINITE DIFFERENCE TEST PROGRAM

In order to test geometries and soil properties not explicitly tabulated by Mitalas, a simple transient heat conduction analysis program was written. This program uses the lumped parameter method because the simple rectangular geometries of basement and slab-on-grade configurations do not require the greater geometric power of the more complex finite element method. Versions of the program were developed for two-dimensional rectangular and cylindrical coordinates and three-dimensional rectangular coordinates. Steady state conduction is solved by Gauss-Seidel iteration. Transient conduction is solved by the standard explicit method. This was chosen instead of an implicit method because of ease of programming and the minimum grid dimensions give a stable solution with time steps no shorter than one-half hour. The experimental comparison data uses a one hour time step, so the simulation cannot use a longer one.

The program allows variable spacing in the finite difference grid which improves accuracy by allowing more detail where the heat flux lines diverge rapidly. Each grid element may be of a different material to describe complex material geometries within the rectangular gird. This freedom of description is simplified by a semi-graphic input as shown in figure 2. This sample input includes the width and height of each grid element, the names (W, C, G, D) and thermal properties of each material, convection coefficients and temperatures, the arrangement of the materials in the grid, the locations where conductive fluxes are computed, and the control values for the output sketches. A sample output page is shown in figure 3 where a simple graphic output of the steady state temperature field allows the user to determine if the results are reasonable. Other output gives the values for conductive heat flux across each of the previously defined areas.

In addition to a simple steady test which produced exact results, the program was tested against a known solution [11] for a semi-infinite solid with periodic boundary conditions which closely resembles heat transfer into undisturbed earth. When the surface of the semi-infinite region has a prescribed periodic temperature of the form

$$T_o = T_{om} \cos(2\pi t/t_o) \qquad (6)$$

where t = time,

t_o = period for one full cycle,

T_{om} = one half the total amplitude of the temperature swing.

The resulting temperature as a function of time and depth, x, into the region is given by

$$T = T_{om} \exp\left(-x\sqrt{\pi/\alpha t_o}\right) \cos\left(2\pi t/t_o - x\sqrt{\pi/\alpha t_o}\right) \quad (7)$$

and the heat flux at the surface at time t is given by

$$Q = kT_{om}\sqrt{t_o/2\pi\alpha}\cos(2\pi t/t_o - \pi/4) \quad (8)$$

where k = thermal conductivity in the region,

α = thermal diffusivity.

Using minimum grid spacings of 0.3 m (1.0 ft) and 0.15 m (0.5 ft), the error in peak heat flux at the surface was found to be 2.9 percent and the error in the phase shift of that peak was 2.2 percent. The uncertainty in knowledge of actual soil thermal properties would usually lead to larger errors.

2.3 THE PASSIVE SOLAR TEST FACILITY

In 1980, the Department of Energy established a Program Area Plan for systematic performance evaluation of passive/hybrid heating and cooling systems [12]. This plan defines three levels of performance monitoring procedures which have been designated, in decreasing order of sophistication, as Class A, B, and C. Class C monitoring involves simple hand-recorded measurements and surveys of occupant reactions. Class A and Class B level monitoring involve fixed instrumentation and data acquisition equipment. Class B monitoring provides limited detailed data (about 20 sensors per building) from occupied buildings for field testing and statistical evaluation of passive systems and buildings. Class A level monitoring provides carefully measured detailed data (about 200 sensors per building) under controlled conditions for use in (1) detailed building energy analysis and model/algorithm validation, and (2) performance characterization of various passive subsystems.

The National Bureau of Standards (NBS), under the sponsorship of DoE, has constructioned a full-scale four-cell passive solar test facility for the purpose of acquiring and distributing Class A level performance data for various passive subsystems. The test facility contains several types of generic passive solar features such as a direct gain system, a collector storage wall (Trombe wall), and clerestory windows. The building is described in detail in the Instrumentation and Site Handbook [13]. A brief description of the building components and instrumentation relative to analyzing earth contact heat transfer follows.

The NBS Passive Solar Test Facility is located in Gaithersburg, Maryland, on an open field with no shading from the surroundings. The building is a rectangular, one-story, slab-on-grade, frame structure with the long axis

running east to west. The floor plan is shown in figure 4. There are four cells of equal floor area and an entry area adjoining cell #1 on the west end of the building. Each cell has a floor area of 30.1 m^2 (324 ft^2) an a total volume of 88.4 m^3 (3122 ft^3).

The floor, a slab-on-grade construction, was designed to be of 102 mm (4 in) of concrete over an equal thickness of gravel on compacted soil. However, the core samples taken from the slab revealed that the slab thickness varies from 120 to 150 mm (4.8 to 6.0 in). The core samples also indicate that the gravel beneath the slab has settled in places, leaving an air gap of up to 30 mm (1.2 in). The measured thermal properties of the slab are a conductivity of 1.42 W/m^oC (0.82 $Btu/hr \cdot ft^oF$), a density of 2240 kg/m^3 (140 lb/ft^3), and a specific heat of 837 J/k^oC (.20 Btu/lb^oF). The exterior walls of cell 3 are of conventional frame construction with an average U-value of 0.36 $W/m^{2o}C$ (0.6 $Btu/ft^2 \cdot hr^oF$). The roof has an average U-value of 0.18 $W/m^{2o}C$ (.031 $Btu/ft^2 \cdot hr^oF$). The windows have a U-value of 3.52 $W/m^{2o}C$ (.62 $Btu/ft^2 \cdot hr^oF$). The clerestory was covered with an insulating shutter during the tests. A total of 457 sensors are installed in and around the building. There are 26 sensors outside the building and 6, 173, 26, and 226 in cells 1 through 4 respectively. There are 20 thermocouples used to monitor the floor surface temperature in cell 3. Figure 6 schematically shows the location of these sensors. The air temperature in cell 3 is monitored at two locations with unshielded thermocouples and averaged. The maximum overall uncertainty in the temperature measurements is estimated to be $\pm$ 0.5 C.

Two short duration performance monitoring experiments were conducted: the first for the period of January 16 to February 13, 1984; and the second from February 17 to March 12, 1984. Results from cells 2 and 4, the collector storage wall and direct gain cells are reported in [14].

Because of the long phase shifts involved in ground heat transfer, weather data are also needed for up to one year prior to the actual test period. This data was obtained from the standard weather data recorded at the Washington, D.C. airport. Comparison between the local weather data and the airport data during the test period indicate that the temperature at the airport averages about 2°C (3°F) warmer than at the Gaithersburg site. So the prior year temperature data has been modified by this amount before being used with the ground heat transfer test program.

3. RESULTS AND DISCUSSION

3.1 COMPARISON TO MITALAS

A further test of the two-dimensional finite difference heat conduction program is obtained by using it to compute the conduction shape factors for two basement configurations which are included in Table 2 of the Mitalas report [9]. The basement geometry is shown in Figure 1. The upper soil has a conductivity of 0.8 $W/m^{o}K$ (.46 $Btu/hr{\cdot}ft^{o}F$) and the lower soil has a conductivity of 0.9 $W/m^{o}K$ (.52 $Btu/hr{\cdot}ft^{o}F$). The soil thermal diffusivity is 6.5 x 10^{-7} m^2/s (0.025 ft^2/hr). A conductivity of 1.73 $W/m^{o}K$ (1.0 $Btu/hr{\cdot}ft^{o}F$) and diffusivity of 0.036 is used for the concrete of the basement to the outside air is important, especially for the top basement wall segment. The results of this test are shown in Table 1 where the values reported by Mitalas are compared with those computed by the finite difference program.

The first basement configuration is uninsulated. The steady-state shape factors, S, are in good agreement for the second and fifth segments, and they differ by -12 percent and -43 percent for the third and fourth segments, respectively. The dynamic shape factors, V, differ by 26 percent, 15 percent, 14 percent, and -40 percent for segments 2 through 5, respectively. The phase shifts, t, measured in months, agree to within 0.6 month. The computed value of V are based on the reported values of , the amplitude attenuation coefficient, which is an average for all configurations and is reported with one digit accuracy. This accuracy, together with the uncertainty in soil diffusivity, indicates a reasonable agreement of two sets of values. In every case, the correct trend for the computed values is obtained.

The second configuration includes insulation on the upper basement wall segment. This insulation significantly reduces the heat loss through the second segment. The values for S differ by -5 percent, -9 percent, -17 percent, and -22 percent for segments 2 through 5 respectively. The values of V differ by +19 percent, +28 percent, +20 percent, and +40 percent. The phase shifts agree to within 0.6 month. Again, the percentage differences are rather large, but all the same trends appear in the reported and the computed data.

3.2 COMPARISON TO MEASURED DATA

Cell #3 of the Passive Solar Test Facility provides over 1100 hours of data for the room air temperature and 20 floor surface temperatures. Figures 7 and 8 show 108 hours of temperature data for the four sensors near the south and north walls respectively. Note that the two figures are different implying that the heat transfer from the floor is not symmetrical. This can reasonably be attributed to differences in construction details and to the solar heating of the earth and foundation at the south of the building while the north side is always in shade. During the entire test period the temperatures on the south side of the floor average .44°C (.79°F) warmer than those on the north side.

Since cell #3 is located near the center for the building, the heat conduction is modeled by the two-dimensional planar finite difference Program. The two sets of thermocouples near the walls provide the

temperatures of narrow strips along the walls while the other twelve thermocouples provide an average temperature for the remainder of the room. The narrow strips comprise 1.3 percent, 1.3 percent, 2.7 percent, and 3.6 percent of the floor area in sequence from the wall to the center of the room for both north and south sides. The central area accounts for 81 percent of the total floor area. The grid structure of the simulation is set up to give heat fluxes and temperatures at points corresponding to the measured area.

The initial computer simulation uses the building thermal properties given in section 2.2. The soil assumed to have values of .90 $W/m^{o}K$ (.52 $Btuhr{\cdot}ft^{o}K$) for conductivity and 6.5 x 10^{-7} m^2/s (0.025 ft^2/hr) for thermal diffusivity. This simulation gives a temperature in the central floor region which is only $0.08^{o}C$ ($.14^{o}F$) higher than the measured values. The root-mean-square error is $0.20^{o}C$ ($.36^{o}F$). This is equivalent to an error of 0.5 W/m^2 (.16 Btu/ft^2) in the heat flux to the ground assuming the floor convection coefficient is 6.13 W/m^2 (1.08 $Btu/hr{\cdot}ft^{2o}F$). However, the predicted temperatures in the thin stripes near the walls average $.74^{o}C$ ($1.3^{o}F$) too high which corresponds to a heat flux error of 4.4 W/m^2 (1.4 $Btu/hr{\cdot}ft^2$). Combining the central and edge areas gives a total error of 1.2 W/m^2 (0.39 $Btu/hr{\cdot}ft^2$) in the predicted ground heat flux. The average error in the rate of energy loss from the floor is 37 w (127 Btu/hr).

From the initial simulation, several changes in the modeling assumptions have been made in order to get the best fit to the measured data. The higher error in the floor edge temperatures than in the center temperature means that ground thermal conductivity cannot account for the entire error. Additional heat losses have to be occurring at the edge of the floor. The simulation is improved by the following assumptions. The thermal conductivity of the ground is increased to 1.07 $W/m^{o}K$ (0.62 $Btu/hr{\cdot}ft^{o}F$). This value is the average of the values used by Mitalas to represent wet and dry soil. The lowest segment of the wall is modeled as if it were solid wood, which represents the wall's base plate, instead of using average thermal properties as in the initial simulation. The insulation on the outside edge of the slab is assumed to have degraded about 50 percent in R-value due to exposure to moisture and poor contact with the wall. And instead of modeling simple convection from the floor to room air, the model was revised to include this component plus radiation to the other room surfaces. These changes should be more accurate models of the heat transfer in the room. Another factor which could cause increased heat loss at the slab edge is infiltration through the point where the wall and the slab meet. This is commonly a significant source of infiltration in homes. The infiltration effect has not been modeled and is, therefore, included to some extent in the other two mechanisms for increased edge loss. These changes produce a simulation where the temperature in the central portion of the floor is in error by only $0.02^{o}C$ ($0.04^{o}F$) over the entire simulation period and the temperatures of the strips near the walls averaged only $0.23^{o}C$ ($0.43^{o}F$) high. These values correspond to a total error of 0.35 W/m^2 (0.11 $Btu/hr{\cdot}ft^2$) in the average heat flux into the ground. The average error in the rate of energy loss from the entire floor of cell #3 is only 10.6 W (36. Btu/hr).

The area averaged measured temperature of the floor is $17.8^{o}C$ ($64.1^{o}F$) during the entire test period. The average room air temperature is $20.7^{o}C$ ($69.2^{o}F$). Therefore, the total heat flux to the ground is computed to be

17.5 W/m^2 (5.54 $Btu/hr \cdot ft^2$). This corresponds to a total energy loss rate of 527 W (1790 Btu/hr). The relative error in heat flux to the ground in the initial simulation is 7.1 percent and in final simulation it is only 2.0 percent. This very good agreement indicates that shape factors generated for the specific configuration would give good annual results for a simple calculation of the heat flux. The difference for hourly or daily heat flux values could be large because of the simplification of the ground surface temperature to a simple harmonic function. The effects of brief periods when the ambient temperature is much above or below the corresponding harmonic value would not be modeled.

3.3 COMPARISON OF 2-D AND 3-D MODELS

The above comparisons to the Mitalas coefficients and the experimental data have involved two-dimensional (2-D) planar ground heat transfer. The data obtained from cell #3 of the Solar Test Facility cannot be used to test three-dimensional (3-D) effects because the measurements occur near the center of the building where 3-D effects are minimal. Therefore, a set of computer simulations described below analyze the importance of 3-D heat conduction into the ground.

A simple rectangular basement geometry is chosen as the base case. Figure 9 shows the finite difference grid used for the heat conduction simulation in two dimensions. Similar grids are used in the extension to three dimensions. The simulation uses variable grid spacing with a minimum grid spacing of 0.3 m (1.0 ft). There is no heat transfer through the above ground portion of the wall. The left and right boundaries are abiabatic -- not heat flux crosses them. This is equivalent to having another identical basement 23.2 m (76 ft) from the basement shown. The deep ground plane is 15.24 m (50 ft) below the ground surface and is maintained at the annual average ground surface temperature. The ground, including the basement wall, has uniform thermal properties with a conductivity of 1.56 $W/m^{2o}K$ (0.90 $Btu/hr \cdot ft^{2o}F$) and a value of 6.5×10^{-7} m^2/s (0.025 ft^2/hr) for the thermal diffusivity. The heat flux into the ground is reported for six areas on the basement wall and floor. A1, A2, A3 are strips 0.61 m (2.0 ft) wide from the top to the bottom of the wall. A4 and A5 are also 0.61 m (2.0 ft) wide strips on the floor; A4 is adjacent to the wall; A5 is inside A4. A6 is the remaining area of the floor -- the part in the center.

Table 2 presents the results of a series of 2-D and 3-D steady-state heat transfer simulations. The heat fluxes are presented for each area, A1 through A6, and the total average heat flux for the entire wall and floor surface of the basement. Case 1 is the results for the 2-D planar simulation of 288 nodes as shown in figure 9. In case 2 a uniform grid size of 0.3 m (1.0 ft) is used instead of the variable grid. The uniform grid with 2670 nodes gives a total heat flux 0.9 percent greater than case 1. In case 3 several of the grid elements adjacent to the basement wall and floor are divided to give a size of 0.15 m (0.5 ft). Using smaller grid elements near the walls gives a total heat flux 2.0 percent greater than case 1. Most of the difference is in the top wall segment -- A1. This result indicates that small grid elements are useful at the point of highest heat flux but do not significantly change the results in a low flux region. However, the change is relatively small and the purpose of the following simulations is comparative only, so the minimum grid spacing in the remaining 2-D and 3-D simulations is 0.3 m (1.0 ft).

Cases 4-3D, 5-3D, 6-3D, and 7-3D present the results for rectangular basements using rectangular three-dimensional simulation with more than 6000 nodes. All four basements are 1.83 m (6.0 ft) deep. Case 4-3D is a square basement 8.53 m (28 ft) on a side. Its total heat flux is 50 percent greater than for case 1. Case 5-3D is a rectangular basement 8.53 m (28 ft) by 17.07 m (56 ft) which are reasonable dimensions for a single family residence. Its total heat flux is 29 percent greater than case 1. Case 6-3D is an elongated rectangular basement 8.53 m (28 ft) wide by 34.14 m (112 ft) long which has a heat flux 15.5 percent greater than case 1. Case 7-3D is a very large square 34.14 m (112 ft) on a side which has a total heat flux 30.7 percent less than case 1. These four cases show both the large effect of the 3-D nature of earth contact heat conduction and the importance of the overall size of the basement on the average heat flux. Note that case 7-3D has heat fluxes in segments A1 through A5 which are very similar to the 2-D model of case 1, and the main difference occurs in the center of the floor. This case cannot be accurately modeled by coefficients which have been generated for a much different basement width such as the values published in [9].

The problem with 3-D simulations is that the calculations are very time consuming. A cube shaped region divided into a N grid points in each direction requires a computation time proportional to N^3. A 2-D simulation requires only N^2 computation time. The simulations above used N=20 which is a minimal value for achieving reasonable accuracy. Therefore the 3-D solution requires about 20 times as much computation time as the 2-D solution. 3-D simulations require about 20 minutes on the NBS mainframe computer. There is another way to model heat transfer into a three dimensional region with the same run time as a 2-D simulation: the 2-D simulation using cylindrical (rather than rectangular) coordinates. But cylindrical coordinates can only be applied to an axi-symmetric configuration. Simulations with a 2-D cylindrical coordinate program and the geometry of case 1 are found to give higher heat fluxes than the 3-D simulation values. The 2-D planar simulation of case 1 gives lower heat fluxes than the 3-D simulations for basements of the same width (cases 4, 5, and 6). This suggests the possibility of combining the 2-D planar and cylindrical simulations in some manner to give results near the 3-D values with much less computational effort.

The geometric interpretation of the best combination procedure is shown in figure 10. A basement with a rectangular floor plan, as shown in the upper figure, is converted to a basement with circular ends, the lower figure. The circular portion is modeled with cylindrical coordinates and the straight section with rectangular coordinates. The geometry is set up to conserve the wall area which is proportional to the perimeter length, P, and the floor area, A, of the basement. The diameter, a, of the circular portion is given by

$$a = (P - \sqrt{P^2 - 4\pi A})/\pi \qquad (9)$$

and the length, b, of the straight portion by

$$b = (p - \pi a)/2 \qquad (10)$$

The depth of the basement is unchanged in this transformation. The heat fluxes from the planar and cylindrical models are combined with proportions

2b and a, respectively, to give the total heat flux from the basement. The idea of a 2-D approximation for 3-D ground heat transfer has been applied before [15], but in that model the basement is assumed to have a cylindrical shape with the floor area held constant. The 2-D approximation developed in this report is much more accurate.

Results using the combined 2-D planar and cylindrical model are presented in Table 2 cases 4-2D, 5-2D, 6-2D, and 7-2D for comparison to the 3-D results. The error in total heat flux is less than 1.5 percent in all cases and the heat fluxes in the individual segments are never in error by more than 2.5 percent. The remaining cases in Table 2 probe the conditions where the 2-D approximation looses accuracy.

In case 8 the distance from the edge of the basement to the outer adiabatic boundary is reduced to 4.9 m (16 ft) which causes the 2-D approximation to over estimate the total average heat flux 1.7 percent. This is not significantly different from the original value in case 5 so it is concluded that interbasement distances greater than about 9 m (30 ft) can be handled by the 2-D approximation. In case 9 the distance to the lower constant temperature surface is reduced to 7.9 m (26 ft) and is found to have no effect on the accuracy relative to case 5 although the total average heat flux is increased by 8.5 percent. In case 10 the soil conductivity is reduced to .90 $Wm^{o}K$ (.52 $Btu/hr{\cdot}ft^{o}F$) and is also found to not change the relative accuracy of the 2-D approximation. Cases 11 and 12 are an H-shaped and an x-shaped basement respectively. In these cases equations (9) and (10) are applied using the perimeter and area which results in the equivalent of a long rectangle. This does not reproduce the primary aspects of the basement geometry, in particular, the degree to which the center of the floor tends to be a long distance from the ground surface as is shown by the increasing errors going from segment A1 to A6.

The 2-D approximation for 3-D earth contact heat transfer is also appropriate for rectangular slab-on-grade configurations. The slab geometry is the same as the basement geometry of figure 9 except the floor is level with the ground surface. There are no wall segments A1, A2, or A3. The results of the simulations are presented in Table 3. Case 1-2D is the result for a 2-D planar simulation. Case 2-3D is a square slab 8.53 m (28 ft) on a side. Its total heat flux is 50 percent greater than case 1. Case 3-3D is a rectangular slab 8.53 m (28 ft) by 17.07 m (56 ft). Its total heat flux is 30 percent greater than case 1. Case 4-3D is an elongated rectangular slab 8.53 m (28 ft) wide by 34.14 m (112 ft) long which has a flux 15 percent greater than case 1. Case 5-3D is a very large square 34.14 m (112 ft) on a side which has a total heat flux 38 percent less than case 1. These cases again show the importance of 3-D heat conduction and overall size on the average heat flux. The 2-D approximation to the 3-D model gives results that are accurate to within 1.7 percent for the total average flux in all four cases. The greatest heat flux errors in any given segment occur in the centers of the square slabs.

Data (which are not shown) for the dynamic heat transfer during the year indicate the same accuracy for the 2-D approximation compared to the full 3-D model as is shown for the steady-state results. This includes both the accuracy of the maximum and minimum annual heat flux values and the phase shifts for the various segments. Therefore, it is concluded that the 2-D

approximation is good for estimating the 3-D heat conduction from rectangular basement and slab-on-grade configurations. The idea of a 2-D approximation for the 3-D effects could be applied in the development of simplified ground heat transfer models or be used directly in detailed building energy analysis simulations.

4. SUMMARY AND RECOMMENDATIONS

This report has shown reasonable agreement between the finite difference test program and the Mitalas method. There is very good agreement between the measured floor surface temperatures of the NBS Passive Solar Test Facility and the temperatures predicted by the test program. These results indicate that shape factors generated for the specific configuration can give good results for a simple calculation of the annual earth contact heat flux. There may be considerable differences in the hourly and daily heat flux values when the actual weather departs from the annual harmonic approximation of the simple method.

A procedure was developed for using 2-D simulation to closely approximate the full 3-D effects of heat transfer from rectangular basements and slabs. The 2-D method requires much less computer time than a 3-D method. The 2-D method can be applied to other numerical procedures for which use a 2-D method for computing earth contact heat flux.

There is a need to incorporate a better ground conduction algorithm into several building energy analysis programs. Since these programs are computer simulations, the algorithm should include the capability of modeling the specific geometry under consideration instead of (or in addition to) using tables of coefficients which have been generated for a manual method. A ground conduction computer algorithm could also include the same weather such as Mitalas' single harmonic function for the earth surface temperature. Interfacing the ground conduction algorithm may still involve problems with time scale matching or generating a true simultaneous solution. Such a ground conduction algorithm should be incorporated into TARP as soon as possible to serve as a demonstration for its use in other building energy analysis programs.

5. ACKNOWLEDGMENTS

This work is sponsored by the Solar Buildings Division, Office of Solar Heat Technology, U.S. Department of Energy, Washington, D.C. 20585, as part of the passive solar energy experimental systems research program.

The author wishes to express his gratitude to Dr. Bal Mahajan for his work with the passive solar test facility and assistance in interpreting the measurements.

6. REFERENCES

[1] Kusuda, T., "NBSLD, the Computer Program for Heating and Cooling Loads in Buildings," National Bureau of Standards (U.S.) Building Science Series 69, July 1976.

[2] Hittle, D. C., "BLAST, the Building Loads Analysis and System Thermodynamics Programs," U.S. Army Construction Engineering Research Laboratory Report TR-E-153, June 1979.

[3] Walton, G. N., "Thermal Analysis Research Program Reference Manual," National Bureau of Standards (U.S.) NBSIR 83-2655, March 1983.

[4] Kusuda,T., Piet, O., and Bean, J. W., "Annual Variation of Temperature Field and Heat Transfer Under Heated Ground Surfaces (Slab-on-Grade Floor Heat Loss Calculations)," National Bureau of Standards (U.S.) Building Science Series 1565, June 1983.

[5] Wang, F. S., "Mathematical Modeling and Computer Simulation of Insulation Systems in Below Grade Application," ASHRAE SP 28, ASHRAE/DoE Conference on Thermal Performance of the Exterior Envelopes of Buildings, Orlando, Florida, December 1979.

[6] Akridge, J. M., and Poulos, J. F., "The Decremented Average Ground-Temperature Method for Predicting the Thermal Performance of Underground Walls," ASHRAE Transactions, Vol. 86, Pt. 2A, 1983.

[7] Yard, D. C., Morton-Gibson, M., and Mitchell, J. W., "Simplified Dimensionless Relations for Heat Loss from Basements," ASHRAE Transactions, Vol. 90, Pt. 1B, 1984.

[8] Swinton, M. C. and Platts, R. E., Engineering Method for Estimating Annual Basement Heat Loads and Insulation Performance," ASHRAE Transactions, Vol. 87, Pt. 2, 1981.

[9] Mitalas, G., "Calculation of Basement Heat Loss," ASHRAE Transactions, Vol. 89, Pt. 1B, 1983.

[10] Poulikakos, D. and Bejan, A., "Penetrative Convection in Porous Medium Bounded by a Horizontal Wall with Hot and Cold Spots," International Journal of Heat and Mass Transfer, Vol. 27, 1984, pp. 1749-1758.

[11] Eckert, E. R.G. and Drake, R. M., Analysis of Heat and Mass Transfer, McGraw-Hill, 1972.

[12] "Program Area Plan: Performance Evaluation of Passive/Hybrid Solar Heating and Cooling Systems," Solar Energy Research Institute Report SERI/PR-721-788, October 1980, Golden, CO.

[13] Mahajan, B. M., "National Bureau of Standards Passive Solar Test Facility - Instrumentation and Site Handbook," National Bureau of Standards (U.S.) NBSIR 84-2911, August 1984.

[14] Mahajan, B. M., "Short Duration Winter-Time Performance of Different Passive Solar Systems," National Bureau of Standards (U.S.) NBSIR 84-2930, August 1984.

[15] Davies, G. R., "Thermal Analysis of Earth Covered Building," Proceedings of the Fourth National Passive Solar Conference, Kansas City, MO, October 3-5, 1979.

Configuration	Variable	Segment n = 2	n = 3	n = 4	n = 5
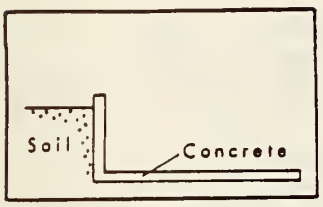	S	1.9	0.74	0.42	0.17
	V	1.9	0.65	0.24	0.05
	σ	0.9	0.7	0.4	0.3
	Δt	0	-1	-2	-4
	C	0	1.0	2.6	0.5
Computed values	S	1.93	0.62	0.33	0.14
	V	2.40	0.75	0.28	0.03
	Δt	0	-.5	-2.6	-3.5
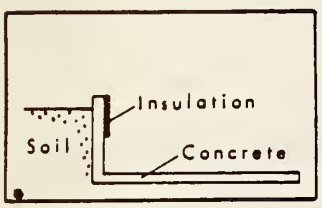 R=1.55	S	0.37	0.96	0.41	0.18
	V	0.36	0.89	0.25	0.05
	σ	0.9	0.7	0.4	0.3
	Δt	0	-1	-2	-4
	C	0	1.0	2.6	0.5
Computed values	S	0.35	0.87	0.34	0.14
	V	0.43	1.14	0.30	0.03
	Δt	0	-0.4	-1.6	-3.5

Table 1. Comparison of Mitalas (S, V, σ, Δt, C) and computed (S, V, Δt) basement heat transfer factors

case	W	L	total	heat fluxes at the indicated basement surfaces A1	A2	A3	A4	A5	A6
1-2D	1	-	1.625	4.423	2.963	2.622	1.769	1.049	0.686
2-2D	1	-	1.640	4.432	2.978	2.640	1.778	1.078	0.698
3-2D	1	-	1.658	4.702	2.982	2.642	1.782	1.043	0.685
4-3D	1	1	2.446	4.651	3.282	3.088	2.265	1.361	0.956
4-2D			2.479	4.716	3.343	3.132	2.266	1.383	0.969
			+1.3%	+1.4%	+1.9%	+1.4%	+0.0%	+1.6%	+1.4%
5-3D	1	2	2.095	4.575	3.176	2.933	2.090	1.240	0.814
5-2D			2.120	4.621	3.220	2.966	2.094	1.260	0.831
			+1.2%	+1.0%	+1.4%	+1.1%	+0.2%	+1.6%	+2.1%
6-3D	1	4	1.877	4.514	3.091	2.809	1.958	1.157	0.746
6-2D			1.893	4.542	3.118	2.829	1.961	1.170	0.758
			+0.9%	+0.6%	+0.9%	+0.7%	+0.2%	+1.1%	+1.6%
7-3D	4	4	1.124	4.447	3.035	2.718	1.848	1.075	0.503
7-2D			1.138	4.497	3.055	2.733	1.847	1.081	0.515
			+1.3%	+1.1%	+0.7%	+0.6%	-0.1%	+0.6%	+2.4%
8-3D	1	2	2.032	4.555	3.129	2.837	1.977	1.163	0.762
8-2D			2.066	4.604	3.181	2.886	2.000	1.194	0.785
			+1.7%	+1.1%	+1.7%	+1.7%	+0.2%	+2.7%	+3.0%
9-3D	1	2	2.273	4.602	3.243	3.092	2.348	1.466	1.048
9-2D			2.304	4.648	3.289	3.129	2.356	1.490	1.078
			+1.4%	+1.0%	+1.4%	+1.2%	+0.3%	+1.6%	+2.9%
10-3D	1	2	1.277	2.924	1.935	1.785	1.257	0.716	0.468
10-2D			1.293	2.953	1.963	1.807	1.260	0.727	0.478
			+ 1.3%	+1.0%	+1.4%	+1.2%	+0.2%	+1.5%	+2.1%
11-3D	H		1.688	4.376	2.936	2.616	1.794	1.040	0.651
11-2D			1.782	4.493	3.058	2.751	1.887	1.121	0.725
			+5.6%	+2.7%	+4.2%	+5.2%	+5.2%	+7.8%	+11.4%
12-3D	X		1.734	4.378	2.949	2.646	1.836	1.062	0.654
12-2D			1.843	4.522	3.092	2.794	1.929	1.149	0.743
			+6.3%	+3.3%	+4.8%	+5.6%	+5.1%	+8.2%	+13.6%

Table 2. Comparison of 3-D and 2-D calculations for a basement configuration, heat flux values in Btu/hrft^2 (x 3.15 gives W/m^2).
W and H indicate the relative width and length of the basement.
("H" and "X" are non-rectangular shapes.)

case	W	L	total	heat fluxes at the indicated slab surfaces A4	A5	A6
1-2D	1	-	1.365	3.540	1.663	0.871
2-3D	1	1	2.055	4.099	2.036	1.236
2-2D			2.066	4.088	2.081	1.297
			+0.5%	-0.3%	+2.2%	+4.9%
3-3D	1	2	1.780	3.902	1.891	1.040
3-2D			1.809	3.893	1.921	1.081
			+1.6%	-0.2%	+1.6%	+3.8%
4-3D	1	4	1.573	3.753	1.791	0.950
4-2D			1.591	3.747	1.810	0.973
			+1.1%	+0.2%	+1.1%	+2.4%
5-3D	4	4	0.848	3.619	1.683	0.557
5-2D			0.863	3.607	1.688	0.575
			+1.7%	-0.3%	+0.3%	+3.2%

Table 3. Comparison of 3-D and 2-D calculations for a slab configuration, heat flux values in Btu/hrft^2 (x 3.15 gives W/m^2).

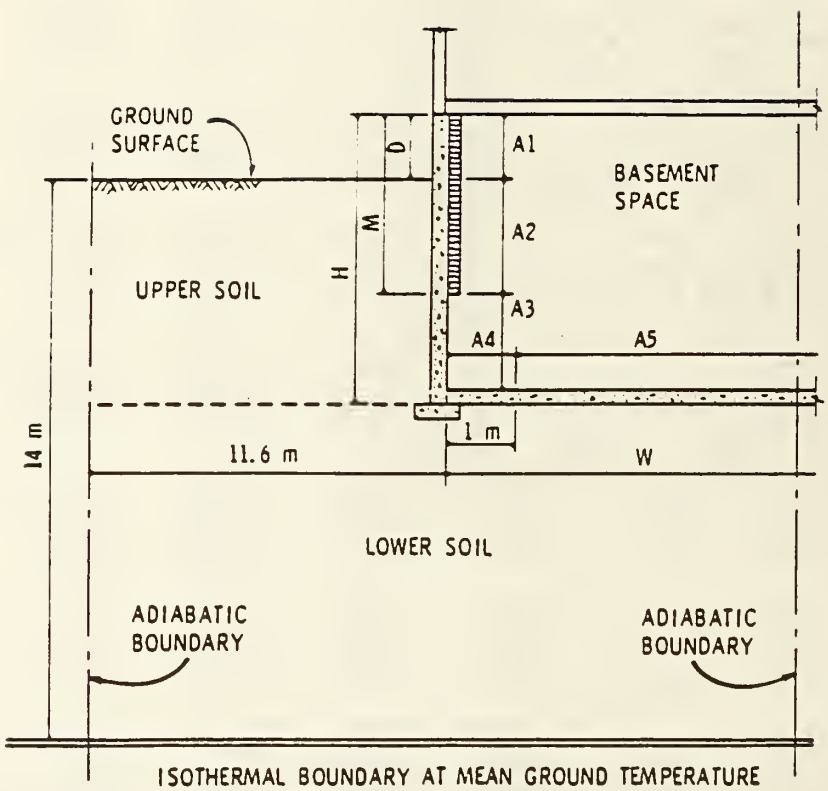

Figure 1. The Mitalas Basement Model

```
SOLAR TEST FACILITY
38 27 0.5 405 4                                                 } run control input
 $OUT DX=1.,3*2.,4*1.,.875,3*.5,4*.25,5*.3333,2*.5,3*1.,4*2.,3*3.,4*4.,1. $END
 $DOWN DY=1.0,3*.5,3*.3333,3*.4167,.6667,2*1,1.0833,3*2.,3*3.,3*4.,4*5. $END
W                                                               } material name
0.0959 13.655 .24                                               } thermal properties
C                                                               } material name
0.82 140. .20                                                   } thermal properties
G                                                               } material name
0.834 55. .40                                                   } thermal properties
D                                                               } material name
0.62 60. .347                                                   } thermal properties
4. 1000. 1.46 1.08                                              } convection values
67.7 0.                                                         } room air temp.
57.6 0. 0.                                                      } outside air temp.
0ZZZZZZZZZZZZZZZZWAAAAAAAAAAAAAAAAAAA0                          } graphic input
0ZZZZZZZZZZZZZZZZWAAAAAAAAAAAAAAAAAAA0                          } of slab/ground
0ZZZZZZZZZZZZZZZZWAAAAAAAAAAAAAAAAAAA0                          } configuration
0CCCCCCCCCCCCCCCCCAAAAAAAAAAAAAAAAAAA0
0GGGGGGGGGGGGGGGCCAAAAAAAAAAAAAAAAAAA0
0DDDDDDDDDDDDDDDCCDDDDDDDDDDDDDDDDDDD0
0DDDDDDDDDDDDDDDCCDDDDDDDDDDDDDDDDDDD0
0DDDDDDDDDDDDDDDCCDDDDDDDDDDDDDDDDDDD0
0DDDDDDDDDDDDDDDCCDDDDDDDDDDDDDDDDDDD0
0DDDDDDDDDDDDDDCCCDDDDDDDDDDDDDDDDDDD0
0DDDDDDDDDDDDDDDDDDDDDDDDDDDDDDDDDDDD0
0DDDDDDDDDDDDDDDDDDDDDDDDDDDDDDDDDDDD0
0DDDDDDDDDDDDDDDDDDDDDDDDDDDDDDDDDDDD0
0DDDDDDDDDDDDDDDDDDDDDDDDDDDDDDDDDDDD0
0DDDDDDDDDDDDDDDDDDDDDDDDDDDDDDDDDDDD0
0DDDDDDDDDDDDDDDDDDDDDDDDDDDDDDDDDDDD0
0DDDDDDDDDDDDDDDDDDDDDDDDDDDDDDDDDDDD0
0DDDDDDDDDDDDDDDDDDDDDDDDDDDDDDDDDDDD0
0DDDDDDDDDDDDDDDDDDDDDDDDDDDDDDDDDDDD0
0DDDDDDDDDDDDDDDDDDDDDDDDDDDDDDDDDDDD0
0DDDDDDDDDDDDDDDDDDDDDDDDDDDDDDDDDDDD0
0DDDDDDDDDDDDDDDDDDDDDDDDDDDDDDDDDDDD0
0DDDDDDDDDDDDDDDDDDDDDDDDDDDDDDDDDDDD0
0DDDDDDDDDDDDDDDDDDDDDDDDDDDDDDDDDDDD0
0DDDDDDDDDDDDDDDDDDDDDDDDDDDDDDDDDDDD0
0DDDDDDDDDDDDDDDDDDDDDDDDDDDDDDDDDDDD0
 $DATA R=3.2,XX=14.0416,Y1=1.5,Y2=3.75 $END                     } insulation
 $DATA R=3.2,YY=3.75,X1=14.0416,X2=15.0415 $END
 $DATA F=1.0,YY=1.5,X1=13.125,X2=13.7083 $END                   } report heat fluxe
 $DATA F=2.0,YY=1.5,X1=12.875,X2=13.375 $END                    } on these surfaces
 $DATA F=3.0,YY=1.5,X1=12.375,X2=12.875 $END
 $DATA F=4.0,YY=1.5,X1=10.875,X2=12.375 $END
 $DATA F=5.0,YY=1.5,X1=0.0,X2=10.875 $END
 $DATA $END
0. 40. .5 0. 46. .83333                                         } specifications for
15 105 195 285 0 0 0 0 0 0 0 0                                  } graphic output
```

Figure 2. A sample input for the 2-D finite difference conduction computer program.

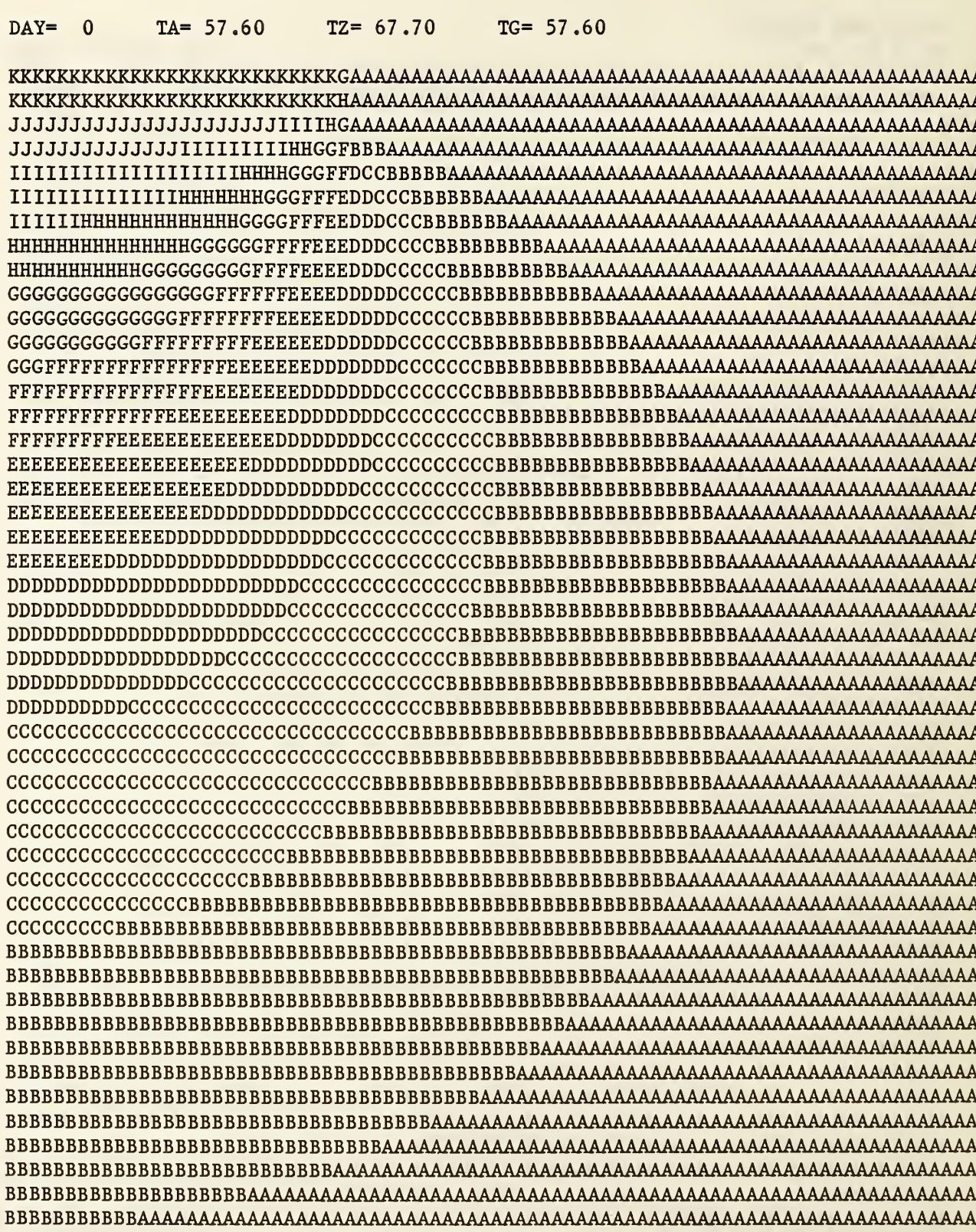

Figure 3. A sample graphic output of the steady state temperature field. Each capital letter is a range 1 degree F warmer than the letter preceeding it (i.e. A = 57.6F to 58.6F, B = 58.6F to 59.6F, ...)

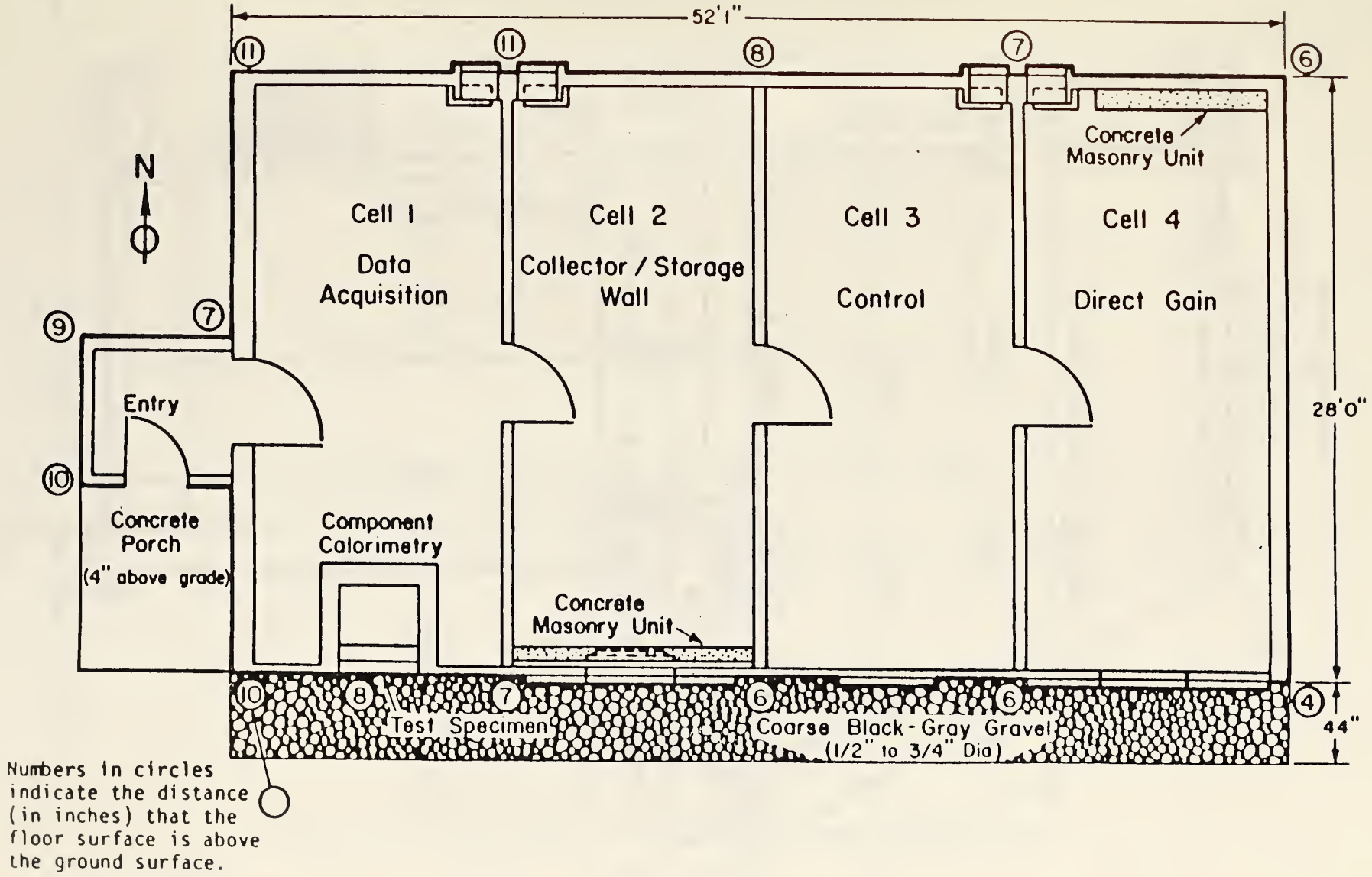

Figure 4. Floor plan of the NBS Passive Solar Test Facility
(Ground heat transfer tests are in cell 3.)

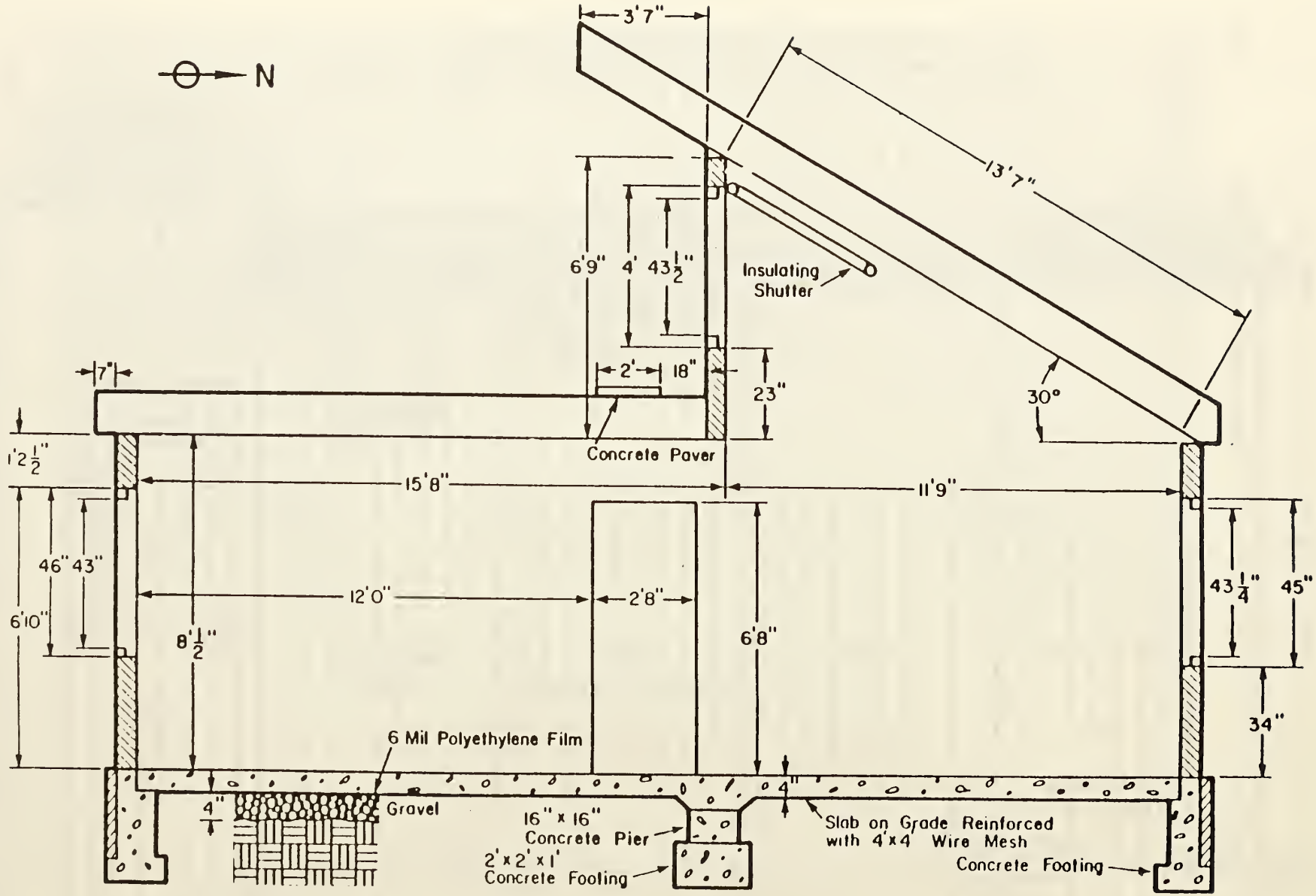

Figure 5. Longitudinal section of Cell #3

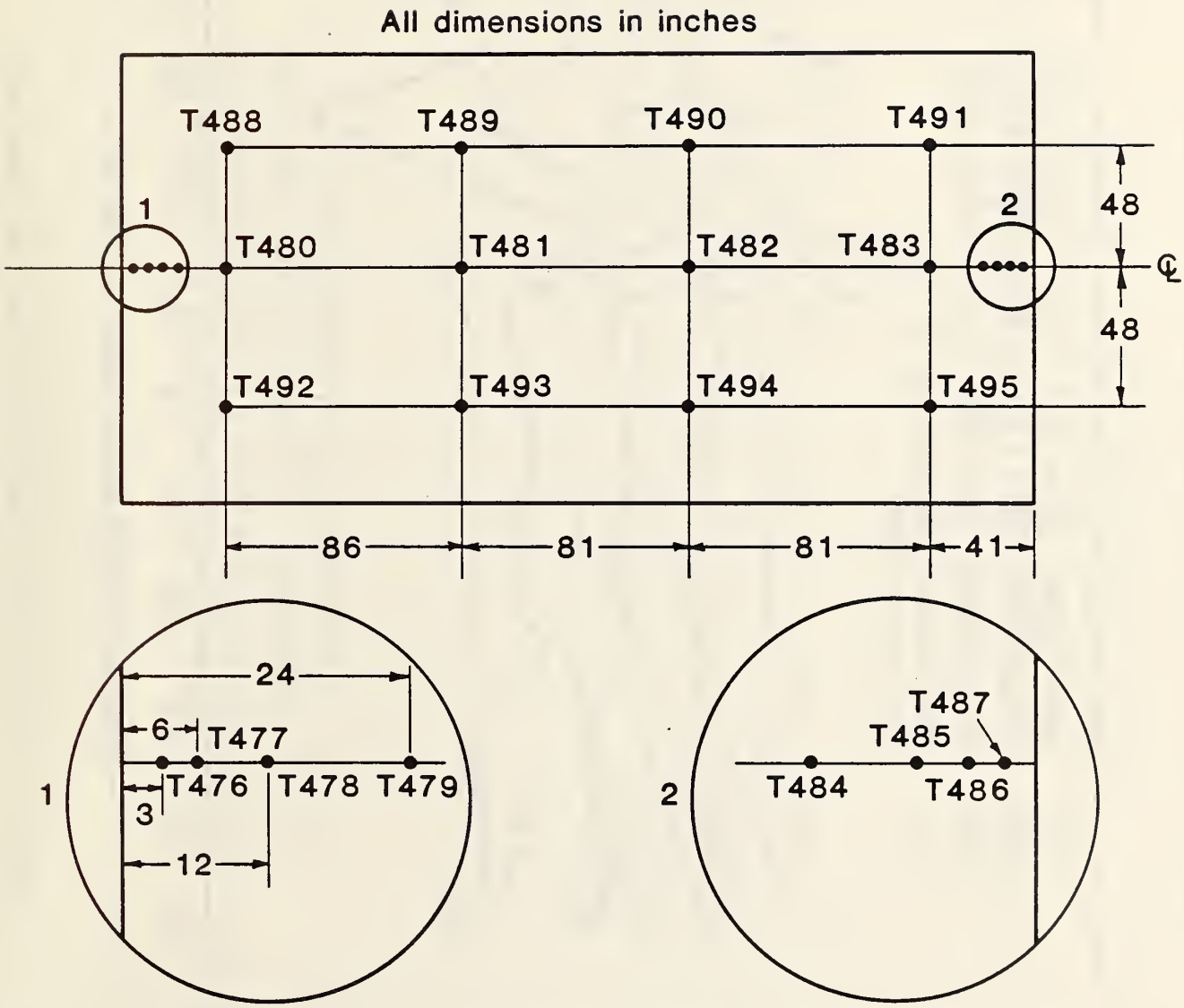

Figure 6. Floor surface temperature sensor locations in Cell 3

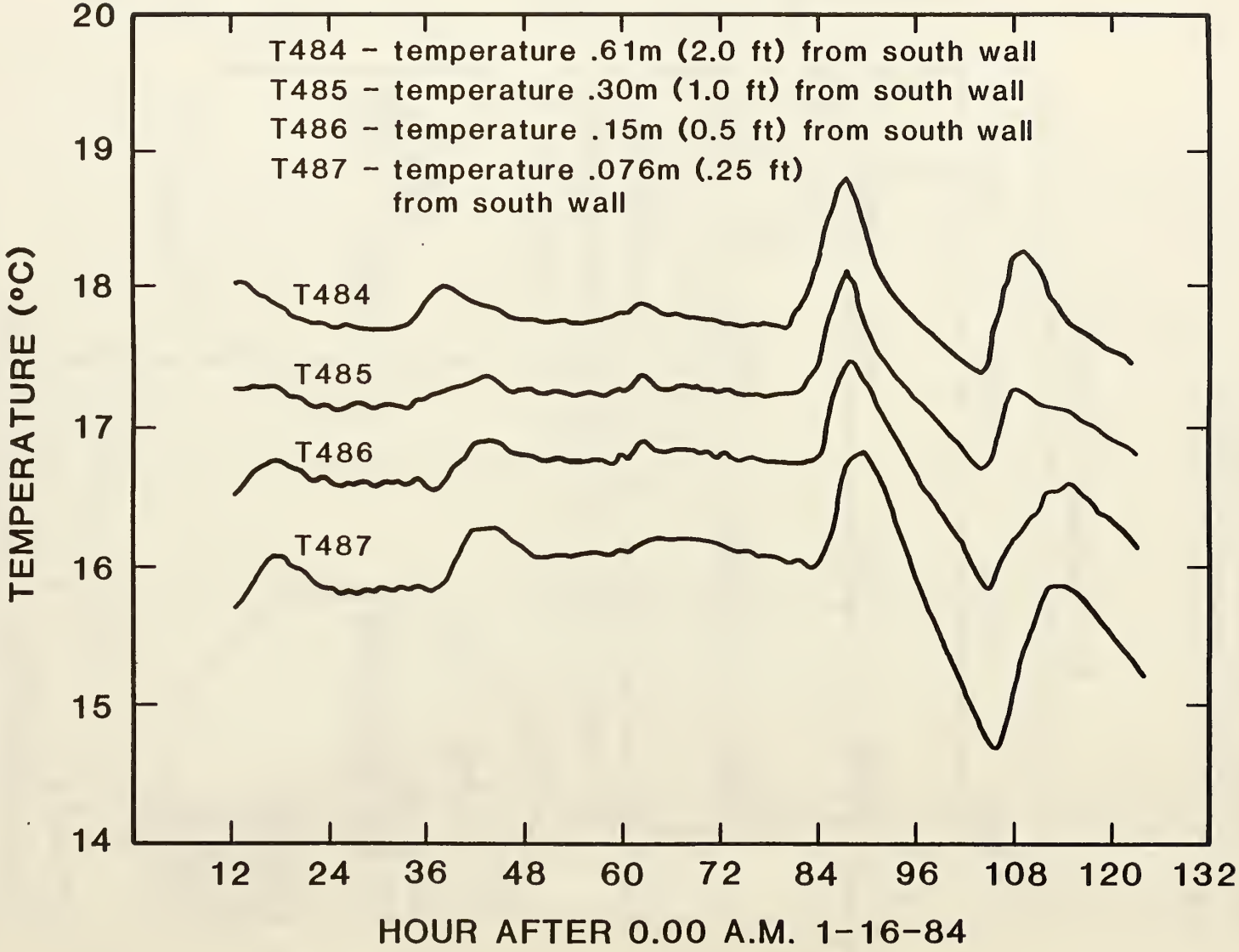

Figure 7. Floor surface temperatures near the south wall

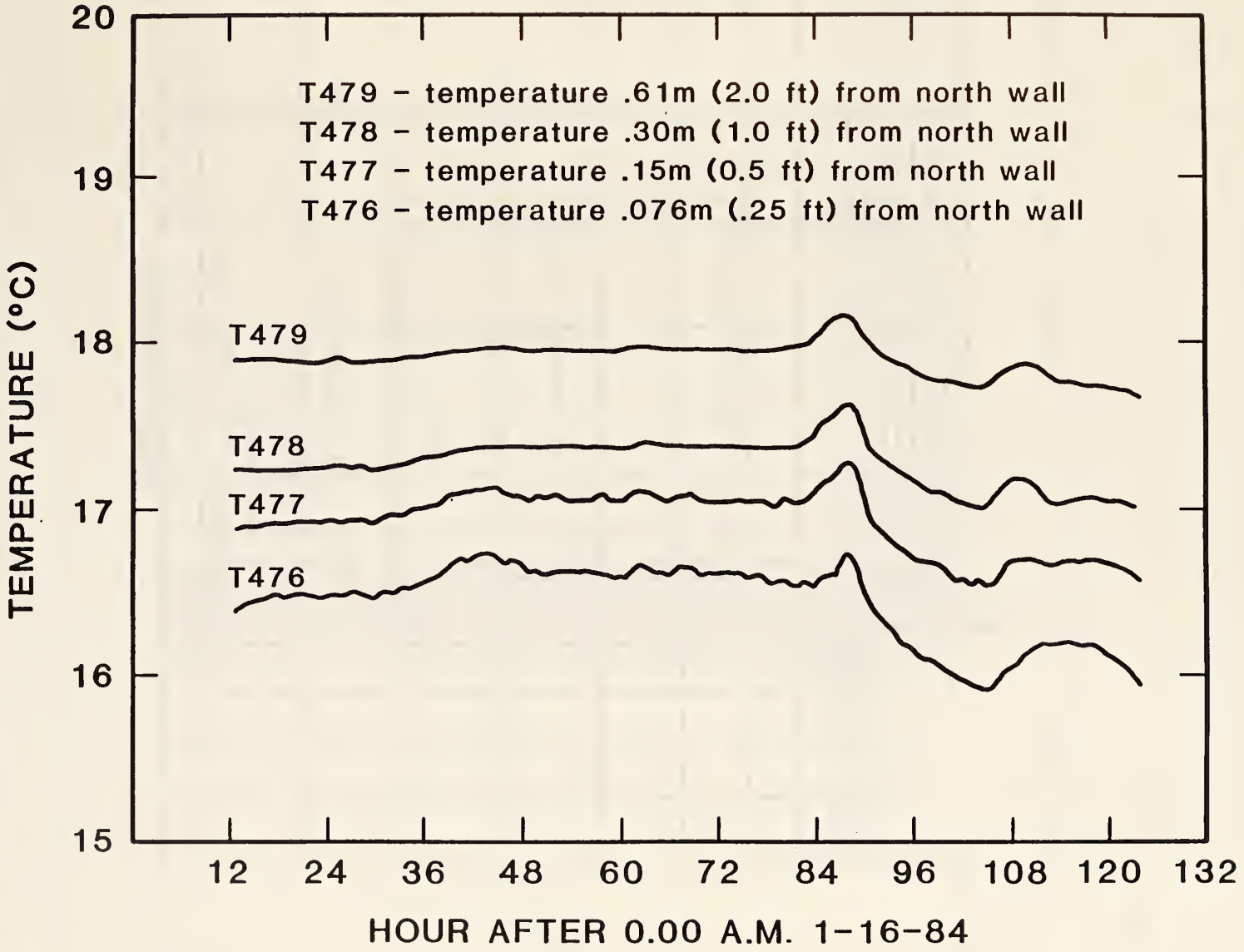

Figure 8. Floor surface temperatures near the north wall

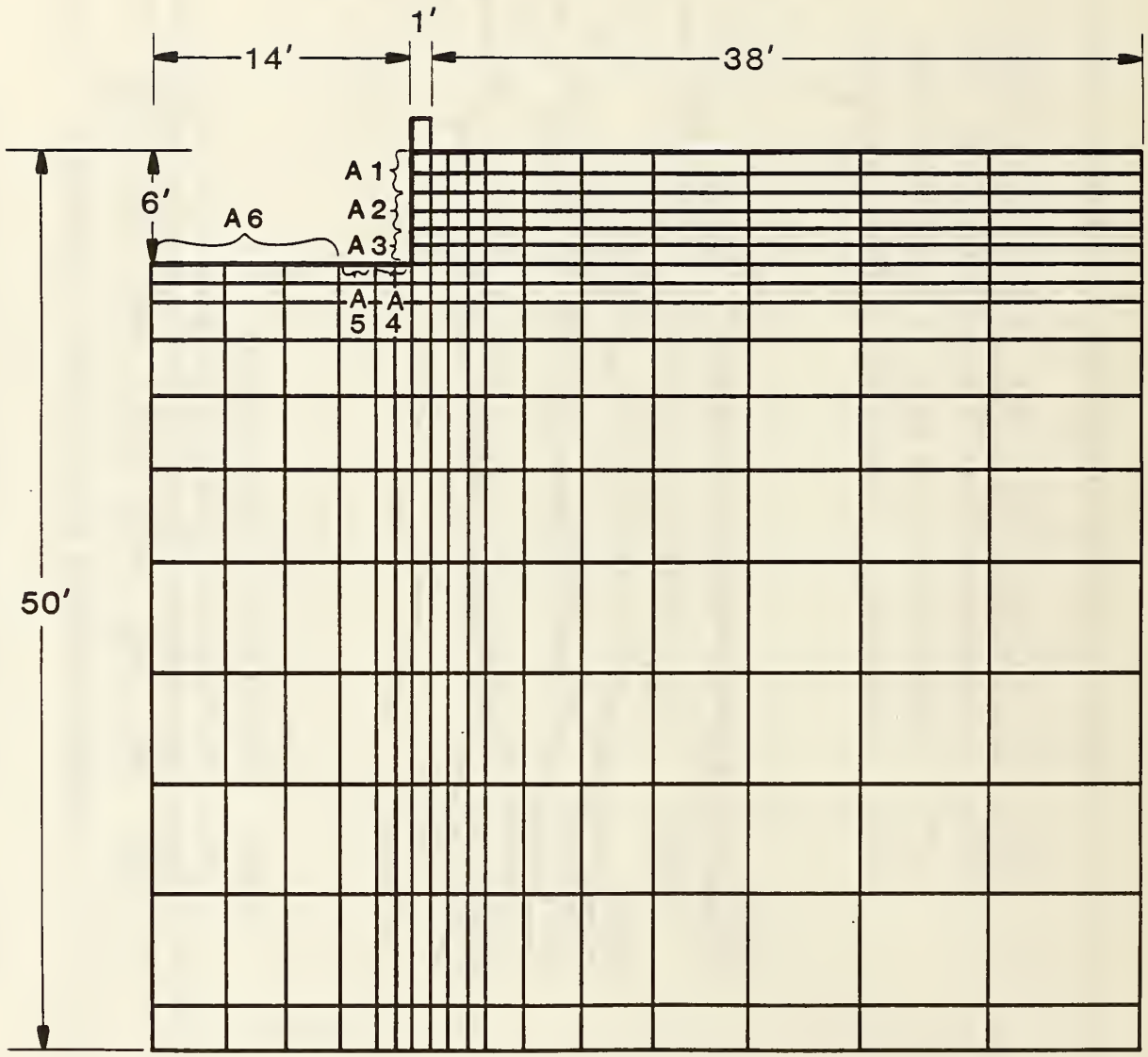

Figure 9. Basic ground configuration for 2-D and 3-D conduction tests

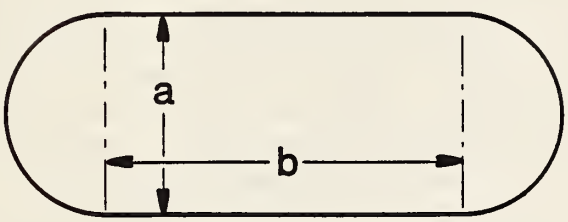

Same perimeter P
Same area A

$$a = (P - \sqrt{P^2 - 4\pi A})/\pi$$

$$b = (P - \pi a)/2$$

Figure 10. 2-D approximation of a rectangular basement or slab

FORM NBS-114A (REV. 11-84)

U.S. DEPT. OF COMM. BIBLIOGRAPHIC DATA SHEET (See instructions)	1. PUBLICATION OR REPORT NO. NBSIR 85-3201	2. Performing Organ. Report No.	3. Publication Date OCTOBER 1985

4. TITLE AND SUBTITLE

Validation Tests of an Earth Contact Heat Transfer Algorithm

5. AUTHOR(S)

George N. Walton

6. PERFORMING ORGANIZATION (If joint or other than NBS, see instructions)

NATIONAL BUREAU OF STANDARDS
U.S. DEPARTMENT OF COMMERCE
GAITHERSBURG, MD 20899

7. Contract/Grant No.

8. Type of Report & Period Covered

9. SPONSORING ORGANIZATION NAME AND COMPLETE ADDRESS (Street, City, State, ZIP)

Solar Buildings Technology Division
Office of Solar Heat Technology
U.S. Department of Energy
Washington, DC 20585

10. SUPPLEMENTARY NOTES

☐ Document describes a computer program; SF-185, FIPS Software Summary, is attached.

11. ABSTRACT (A 200-word or less factual summary of most significant information. If document includes a significant bibliography or literature survey, mention it here)

Experimental tests and numerical calculations are performed to determine the suitability of including a simplified earth contact heat transfer algorithm in building energy analysis computer simulations. Reasonable agreement is shown between the finite difference test program and the simplified method. There is very good agreement between the floor surface temperature of the NBS Passive Solar Test Facility and the temperature predicted by the test program. These results indicate that simplifications based upon the specific configuration can give good results for a simple calculation of the annual harmonic approximation of the simple method. A procedure is developed for using two-dimensional (2-D) simulation to closely approximate the full 3-D effects of heat transfer from rectangular basements and slabs. The 2-D method can be applied to other numerical procedures for which use a 2-D method for computing earth contact heat flux. It is recommended that any algorithm used in a large building energy analysis computer program include the capability of modeling the specific geometry under consideration instead of (or in addition to) using tables of coefficients which have been generated for a manual method. The algorithm should also include the ability to handle the same weather data that is used in the energy analysis.

12. KEY WORDS (Six to twelve entries; alphabetical order; capitalize only proper names; and separate key words by semicolons)

Earth contact heat transfer; building energy analysis, computer simulation; ground conduction; basement heat loss, slab-on-grade heat loss

13. AVAILABILITY

☒ Unlimited

☐ For Official Distribution. Do Not Release to NTIS

☐ Order From Superintendent of Documents, U.S. Government Printing Office, Washington, DC 20402.

☒ Order From National Technical Information Service (NTIS), Springfield, VA 22161

14. NO. OF PRINTED PAGES

34

15. Price

$9.95